Available online at www.sciencedirect.com

ScienceDirect

Ceramics International 40 (2014) 249–256

CERAMICS INTERNATIONAL

www.elsevier.com/locate/ceramint

# Influence of citrate/nitrate ratio on the preparation of $Li_{0.5}La_{0.5}TiO_3$ nanopowder by combustion method

Carlos. R. Milian Pila[a], Teobaldo Mariño Otero[a], Eduardo Pérez Cappe[a], Oswaldo Luiz Alves[b], Pilar Aranda[c], Miguel Aguilar Frutis[d], Yodalgis Mosqueda Laffita[a,*]

[a]*Institute of Materials Science and Technology, Havana University, 10400 Havana, Cuba*
[b]*Instituto de Química, Universidade Estadual de Campinas, UNICAMP, Brasil*
[c]*Instituto de Ciencia de Materiales de Madrid, CSIC, Cantoblanco, 28049 Madrid, Spain*
[d]*CICATA-IPN, Legaria 694, Col. Irrigación, Del. Miguel Hidalgo, C.P. 11500, México*

Received 9 March 2013; received in revised form 4 May 2013; accepted 27 May 2013
Available online 13 June 2013

**Abstract**

Preparation of nano-crystalline $Li_{0.5}La_{0.5}TiO_3$ perovskite material using citrate–nitrate redox reaction by the combustion technique is reported. The role of the ammonium nitrate concentration used to co-precipitate the $Li_{0.5}La_{0.5}Ti$-citrate precursor is revealed by ATD/TG, XRD, SEM-EDX and HRTEM techniques. Thermo-gravimetric analysis data show how the intensity of the exothermic peak associated with the citrate–nitrate redox reaction decreases until disappearance as the citrate/nitrate molar ratio increases. The XRD study indicates that a single-phase cubic $Li_{0.5}La_{0.5}TiO_3$ phase is formed at 350 °C when the citrate/nitrate ratio varies between 0.13 and 0.17. The formed $Li_{0.5}La_{0.5}TiO_3$ powders show an average particle size of 15–20 nm. Electrochemical impedance spectroscopy technique reveals a relative high ionic conductivity inside the grain for the nanometric $Li_{0.5}La_{0.5}TiO_3$ material, with values of around $10^{-4}$ S/cm at room temperature.


*Keywords:* A. Powders: chemical preparation; C. Impedance; D. Perovskite; E. Batteries

## 1. Introduction

In the last 30 years much work has been carried out in order to improve the behavior of rechargeable lithium batteries [1,2]. In this context, both the search of new solid ionic conductors (SIC) and the improvement of its high lithium conductivity at room temperature, usually conditioned by the presence of open-frameworks and particles of nanometric size, are key target points in the current research [3,4]. Amongst other inorganic solids, those related to the perovskite-type materials of the $Li_{3x}La_{2/3-x}TiO_3$ ($\sim 0.04 < x \leq 0.16$) solid solution system, usually called LLTO, attract increasing interest as SIC. Actually several of these materials show the highest values of Li conductivity at room temperature measured in a SIC till the present [5,6].

LLTO compounds have been traditionally synthesized by the ceramic method, which presents as fundamental handicap the necessity of heating at high temperature (900–1300 °C) the precursors for large periods of reaction time (24–48 h) to reach the formation of the desired phase. Therefore, the use of such drastic experimental conditions does not allow a well control of the final stoichiometry [7,8] and, often this drives to the formation of materials that show particles of relative big size. In this way, methods of synthesis that may drive to the formation of nanoparticulated materials are gaining more and more importance. Amongst them the sol–gel method [7,8] and its variants [9–11] have been already employed to prepare LTTO materials. These methodologies make possible to obtain the perovskite phase in the 800 °C–1200 °C temperature range with formation of particles of around 100 nm average sizes. However, these routes very often involve multiple steps processes and the use of expensive starting reagents. Moreover, in some cases they lead to the formation of mixture of phases as well as to the presence of $Li_2Ti_2O_5$ and $TiO_2$ impurities, making

*Corresponding author. Tel.: +53 7 8707666; fax: +53 7 8707898.
*E-mail addresses:* yodalgis@imre.oc.uh.cu, barlomepardo@gmail.com (Y.M. Laffita).

0272-8842/$ - see front matter © 2013 Elsevier Ltd and Techna Group S.r.l. All rights reserved.
http://dx.doi.org/10.1016/j.ceramint.2013.05.131

worth the search of alternative and more efficient routes of synthesis. Thus, the combustion method that profits from the heat generated in the citrate–nitrate redox reaction has been successfully employed in the preparation of numerous ceramic materials, such as $La_{.8}Sr_{0.2}CrO_3$, SiC, TiC, Fe–Cr oxides, $La_{1-x}Sr_xMnO$ and YSZ [12–20], in the form of nanoparticles. Nevertheless, this approach has been only very recently applied by our group to prepare materials of the LLTO system [21]. In this first work it was reported the preparation of $Li_{0.48}La_{0.50}TiO_3$ nanoparticles without $La_2Ti_2O_7$ and $Li_2Ti_2O_5$ impurities from a new mixed-citrate precursor of Li–La–Ti. Interestingly, in that work it was also found that the thermal behavior of the citrate precursor was strongly conditioned by the procedure used to precipitate the precursor from a solution of Li–La–Ti cations that also contained citrate and nitrate ions with molar ratio of 1:1:2:2:9, respectively. The formation of a certain amount of ammonium nitrate that co-precipitated with the precursor seemed to be the reason for the observed decreasing in the LLTO formation temperature although a clear explanation of the phenomenon was not given. Following with this research, in the present work we introduce new results that intend to clarify the relationship between the initial composition and thermal transformation mechanisms of several solid Li–La–Ti-citrate/ammonium nitrate precursors and the final characteristics of the LLTO phase. The final aim is to understand and so, to control, the reaction process in order to obtain nanoparticles of the $Li_{0.5}La_{0.5}TiO_3$ phase without inorganic impurities at very low temperatures.

## 2. Experimental

### 2.1. Preparation of the mixed Li–La–Ti–Cit–Nit precursors and its resulting oxides

The lithium-lanthanum-titanium-citrate/ammonium nitrate precursors (*Li–La–Ti–Cit–Nit*) were synthesized by the previously reported route described elsewhere [21]. Briefly, titanium as metallic powder (Fluka) was dissolved in a mixture of a $H_2O_2/NH_4OH$ aqueous solutions (Merck), then pure citric acid (Merck) was drop wise added to that mixture to reach a 1:1 $C_2H_8O_7$/Ti proportion. The $Li^+$ and $La^{3+}$ ions were introduced to this system by addition of $Li_2CO_3$ (Merck) and $La_2CO_3$ (Merck) dissolved in $HNO_3$ (Merck) in a 0.5:0.5:9 Li:La:$NO_3^-$ stoichiometric ratio. Afterwards, the pH of the final mixture of components was adjusted to a basic value by adding $NH_4OH$ (25% aqueous solution, Merck). In the present case different amounts of $NH_4NO_3$ can be incorporated to the final citrate precursors by further adding of $HNO_3$ (30%) at variable concentration (0, 0.5, 1, 3 and 5.6 M) to the precursor solution. The final citrate precursors containing variable amounts of co-precipitated $NH_4NO_3$ were recovered after solvent evaporation.

The obtained mixed-citrate/nitrate precursors were characterized by different physical-chemical techniques and then thermally treated at 350 °C, 450 °C, 600 °C and 800 °C for 6 h in order to form the LLTO phase and then explore the influence of the $NH_4NO_3$ content in the characteristics of the $Li_{0.5}La_{0.5}TiO_3$ material formed in each case.

### 2.2. Characterization

Powder X-ray diffraction (XRD) patterns of Li–La–Ti–Cit–Nit precursors and final oxide phases were recorded in a Shimadzu XRD7000 diffractometer, using Cu-$K_\alpha$ radiation with a $\Delta 2\theta = 0.02°$ in the 10° to 90° $2\theta$ range. Phase identification in the recorded patterns was carried out by using the Hanawalt method and the PDF-2002 and ICSD-2008 databases. Differential thermal analysis (DTA) and thermogravimetric (TG) curves were obtained in a TGA SDTQ600 TA Instrument analyzer applying a 5 °C $min^{-1}$ heating rate from room temperature to 900 °C in static air. The infrared spectra (FTIR) in the 400–4000 $cm^{-1}$ region were recorded in samples prepared as diluted KBr pellets using a FTLA-2000 spectrometer. CHN elemental microanalyses of the precursors were carried out in a Perkin Elmer 2400 equipment. Samples were studied by high-resolution transmission electron microscopy (HRTEM) in a JEOL JEM-2200FS equipment provided with Schottky type field emission gun operating at 200 kV. The point resolution was of 0.19 nm and the information limit was better than 0.10 nm. HRTEM digital images were obtained using a CCD camera and Digital Micrograph Software from GATAN. Electrochemical impedance spectroscopy (ESI) measurements were carried out using a frequency response analyzer (Solartron SI1260) coupled to a potentiostat/galvanostat (Princeton Applied Research PAR 273A), applying a 200 mV amplitude signal over the frequency range of 10 Hz–10 MHz, recording spectra in the 25–400 °C temperature range. For this study, the samples were prepared as thin pellets pressed at 10 MPa and covered with silver paint on both faces to ensure a tight contact with the Pt electrodes.

## 3. Results and discussion

To study the influence of $NH_4NO_3$ present in the Li–La–Ti–Cit–Nit precursors in the formation of a pure $Li_{0.5}La_{0.5}TiO_3$ oxide phase we have here prepared five Li–La–Ti citrate precursors (with a 0.5:0.5:1 Li:La:Ti ratio) co-precipitated with different $NH_4NO_3$ content. From the CHN elemental microanalysis of the precursors it is possible to corroborate the presence of C and N in the precipitates (Table 1), which correspond approximately to the quantities expected for the formation of a mixed citrate phase with a precipitate of $NH_4NO_3$. The interesting point here seems to be the presence of nitrogen in PCit-1, where $NH_4NO_3$ was not co-precipitated. This apparently contradiction is clarified from IR spectroscopy data (Fig. 1) where identification of functional groups in the phases precipitated for each precursor solution has been analyzed. The presence of nitrogen in PCit-1 is attributed to the ammonium citrate formed during the synthesis. This is corroborated by the presence of the band at 3183 $cm^{-1}$ assigned to the asymmetric stretching vibration band of the ammonium ion [22]. Unfortunately, the band corresponding to the in plane bending vibration of ammonium ion at 1384 $cm^{-1}$ is not observed because it is superimposed by the most intense band of the symmetric vibration mode of the carboxilate groups at around 1400 $cm^{-1}$. Though, in the IR spectra of the PCit-2, PCit-3, PCit-4 and PCit-5 precursors (Fig. 1) are observed the same bands detected

Table 1
CHN content in the Li–La–Ti-Cit-Nit precursors.

| Citrate precursor | C (%) | N (%) | H(%) |
|---|---|---|---|
| PCit-1 | 16.9 | 8.9 | 5.1 |
| PCit-2 | 11.1 | 10.7 | 3.3 |
| PCit-3 | 11.3 | 11.2 | 3.2 |
| PCit-4 | 6.2 | 17.8 | 3.4 |
| PCit-5 | 7.8 | 22.3 | 4.2 |

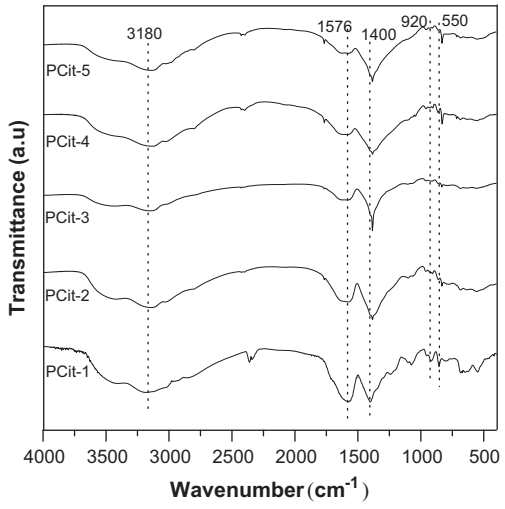


Fig. 1. IR spectra of PCit-1, PCit-2, PCit-3, PCit-4 and PCit-5 citrate precursors.

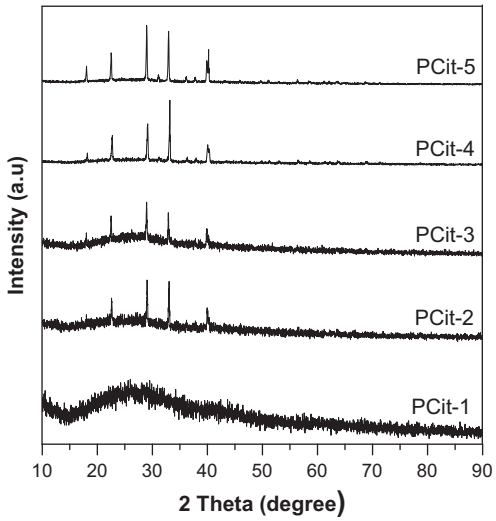


Fig. 2. XRD patterns of PCit-1, PCit-2, PCit-3, PCit-4 and PCit-5 citrate precursors.

in the one of the PCit-1 precursor, their intensities are diminished in comparison due to the presence of the very strong vibrational band about 1385 $cm^{-1}$ characteristic of $\upsilon_{as}$ ($NO_3^-$) [22]. In the IR spectra of all the prepared precursors are observed two bands at 1576 $cm^{-1}$ and 1400 $cm^{-1}$, corresponding to the antisymmetric and symmetric stretching vibration modes characteristic of carboxylate groups [23,24], respectively, confirming the presence of citrate ions in all the precursors. Around 850 $cm^{-1}$ and 920 $cm^{-1}$ are observed vibration bands that can be assigned to stretching vibration modes of –O–O– bonds in coordinated peroxo group. Additionally, it is observed bands around 550 $cm^{-1}$ and 625 $cm^{-1}$ that can be ascribed to the symmetric and antisymmetric stretching vibration bands of Ti–$O_2$ group, respectively. The presence of these two last types of bands could be related to the existence of a certain degree of interaction between Ti (IV) and peroxide groups formed as the titanium metal is dissolved and oxidized due to the action of the hydroxide peroxide as it has been reported elsewhere [25–28].

The XRD (Fig. 2) patterns of the Li–La–Ti–Cit–Nit precursors show relevant differences between PCit-1 and all the other precursors. Thus, the diffractogram of the PCit-1 precursor shows a broad signal between 20° and 40° in 2$\theta$ with an appreciable noisy background, which is characteristic of amorphous compounds. In contrast the XRD patterns of the other precursors (PCit-2, PCit-3, PCit-4 and PCit-5) only show the characteristic XRD profile of $NH_4NO_3$ (chart 24013 of ICSD-2008) overimposed to the background of an amorphous material. It should be noted that the intensity of the XRD peaks assigned to $NH_4NO_3$ increases for compounds prepared with $HNO_3$ solution of higher concentration. Considering the CHN elemental microanalysis data and both XRD and IR results most probably the precursors, except PCit-1, are composed of a mixture of citrateperoxotitanate (IV) species and $NH_4NO_3$.

In Fig. 3 are collected the TG-DTA curves of the 5 precursors grouped in three separated graphics, showing clearly three types of thermal behavior. In the case of the PCit-1 precursor (Fig. 3A) it could be identified five different thermal steps accompanied of weight losses. A first endothermic process between 25 °C and 166 °C (*step a*) that is accompanied by a weight loss (approximately 9%), which can be assigned to the loss of four water molecules solvated in the solid. From 166 °C to 222 °C (*step b*) there is an endothermic peak centered at 188 °C which is accompanied by a big weight loss (approximately 21%).These processes can be ascribed to the $NH_3$ evolution from the solid and the well known successive transformation of citrate ($C_6H_8O_7$) firstly into aconitic acid ($C_6H_6O_6$) by elimination of water molecule [23,27,29], later into itaconic acid ($C_5H_6O_4$) by means of a decarboxilation reaction till a final loss of water during its last transformation in citraconic anhydrade ($C_5H_4O_3$) [30,31]. The endothermic effect between 232 °C and 431 °C (*step c*) is accompanied by a weight loss of 28% that can be ascribed to the decomposition of $C_5H_4O_3$ species producing

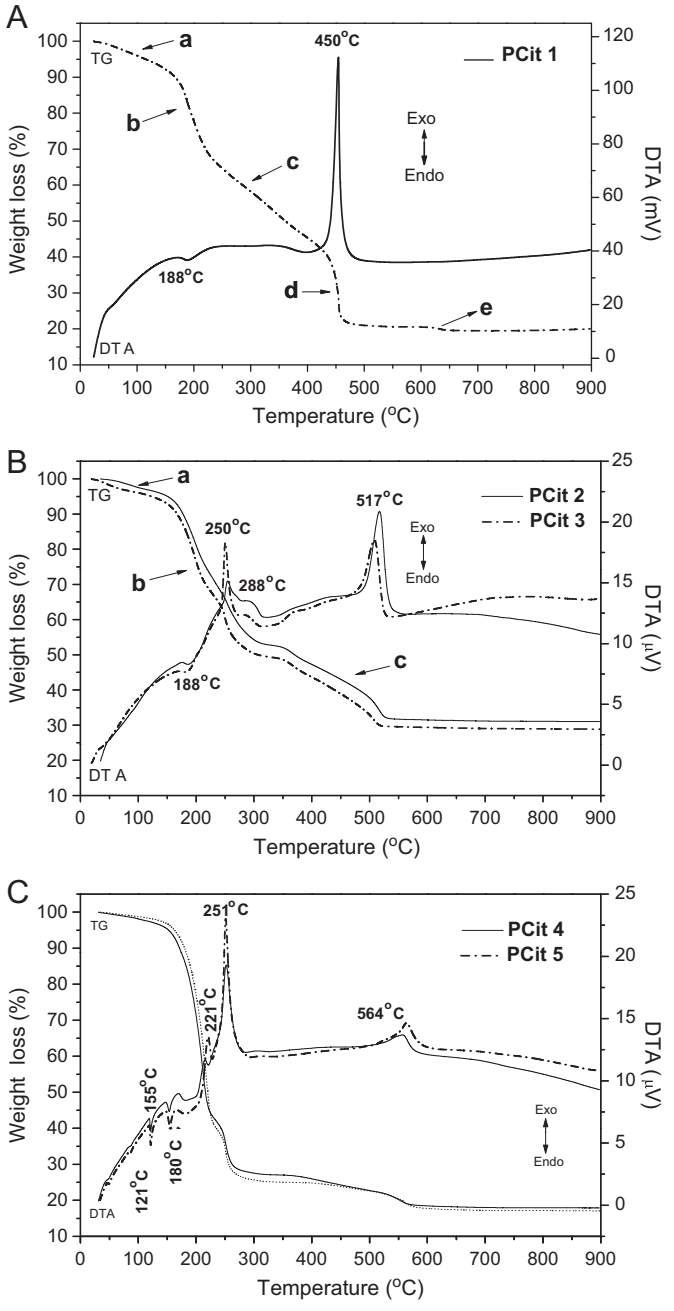


Fig. 3. The TG and DTA curves of (A) PCit-1, (B) PCit-2 and PCit-3, (C) PCit-4 and PCit-5 (heating from 25 °C to 900 °C in air).

$H_2O$, $CO_2$ and/or CO molecules. The most relevant thermal effect corresponds to an intense exothermic process at around 454 °C (*step d*), which is accompanied by a weight loss of approximately 20% related to the combustion of the organic matter. Finally, the small thermal effect at around 640 °C (*step e*) that is accompanied by a weight loss (approximately 1%) was assigned to the elimination of residualorganic matter.

The thermal behavior of the other precursors is very singular and different to that of the PCit-1. It was found that it is strongly dependent of the final $NH_4NO_3$ content which is related to the citrate/nitrate (C/N) ratio in the starting solution. According to that, the PCit-2, PCit-3, PCit-4 and PCit-5 curves could be separated and analyzed in two distinct groups, as illustrate in Fig. 3B and C.

The thermal behavior of PCit-2 and PCit-3 presents three fundamental steps (see Fig. 3B). Between 20 and 170 °C (*step a*) is observed the dehydration of precursors with a weight loss of around 9%. As temperature increases, a loss of weight of around 43.5% between 170 °C and 305 °C is observed (*step b*). In this step are combined (i) an endothermic effect at around 190 °C associated with the transformation of the citrate ions into aconitate, and (ii) two exothermic effects at around 250 °C and 290 °C associated with redox reactions between the precipitated ammonium nitrate and organic matter present in the precursors [12]. It is observed a third region (step *c*) characterized by a strong exothermic event at around 515 °C that is accompanied by a big weight loss (approximately 20%), which can be related to the combustion of residual organic material in air. Typical phase transitions and melting process associated with the presence of ammonium nitrate salts cannot be observed probably due to the low concentration of this salt in these precursors.

The thermal behavior of PCit-4 and PCit-5 precursors (Fig. 3C) also can be described grouping in three main steps. Between 25 °C and 160 °C (*step a*) is again observed a weight loss of around 8% that can be o attributed to the partial dehydration of the precursors. In the curves of these compounds it is also observed two other endothermic peaks at around 120 °C and 155 °C, respectively, that in these cases can be associated with the well-known phase transitions of $NH_4NO_3$ [32–34]. In the second step defined between 160 °C and 350 °C (*step b*) it can be observed an abrupt weight loss of 66% which is accompanied by several thermal events. The first one between 170 °C and 200 °C is a broad endothermic effect that can be related to the melting process of ammonium nitrate (170 °C) and the transformation of the citrate ions into aconitate (typically appearing near to 180 °C). At 220 °C takes place a small exothermic effect that precedes to a more energetic effect ascribed to the intense and narrow peak at around 260 °C. These effects can be attributed to the redox reaction (combustion) between the nitrate and the matter organic [10,12,35]. Finally between 350 °C and 590 °C (*step c*) it is observed a small exothermic process at around 565 °C which is accompanied by a weight loss of about 8% which is again attributed to the decomposition of the residual organic matter in air, as in the other studied precursors.

Table 2 summarized the compositions and calculated citrate nitrate ratio ($\psi$) of all the prepared precursors. Here were evaluated all the results obtained up to now considering the following highlight: (1) the main phase at the end of the thermal analysis is $Li_{0.5}La_{0.5}TiO_3$ as has been corroborated by XRD, and (2) the initial precursor in all the cases has to be electrically neutral. In addition, it must be signaled that during the PCit-1 synthesis an excess of citric acid has been used to warrant the dissolution of the initial carbonates. In all the precursors, it can be assumed the formation of $Li_{0.5}La_{0.5}[Ti(O_2)(C_6H_4O_7)]$ complexes where $Li^+$ and $La^{3+}$ cations are neutralizing the charge of $[Ti(O_2)(C_6H_4O_7)]^{2-}$ anions.

Table 2
Composition of Li–La–Ti–Cit–Nit precursors.

| Citrate precursor | Composition | Calculated citrate/nitrate ratio ($\Psi$) |
|---|---|---|
| PCit-1 | $(NH4)_4$ $Li_{0.5}La_{0.5}Ti(O_2)(C_6H_4O_7)_2{\cdot}4H_2O$ | ∞ |
| PCit-2 | $Li_{0.5}La_{0.5}Ti(O_2)(C_6H_4O_7){\cdot}3H_2O$ 2.2 $NH_4NO_3$ | 0.50 |
| PCit-3 | $Li_{0.5}La_{0.5}Ti(O_2)(C_6H_4O_7){\cdot}3H_2O$ 2.5 $NH_4NO_3$ | 0.40 |
| PCit-4 | $Li_{0.5}La_{0.5}Ti(O_2)(C_6H_4O_7){\cdot}4H_2O$ $6NH_4NO_3$ | 0.17 |
| PCit-5 | $Li_{0.5}La_{0.5}Ti(O_2)(C_6H_4O_7){\cdot}4H_2O$ $7.5NH_4NO_3$ | 0.13 |

The thermal study demonstrates that the presence of ammonium nitrate co-precipitated with the $Li_{0.5}La_{0.5}[Ti(O_2)(C_6H_4O_7)]$ particles provokes enough heat in its decomposition to speed up the oxidation process of the organic phase present in the precursor towards the formation of the oxide phase. In this way the transformation starts at around 260 °C, much lower temperatures, than the typical 450 °C at which the reaction occurs when ammonium nitrate is absent. This redox reaction between the organic matter and nitrate species is very exothermic and the evolved heat depends on the citrate/nitrate molar ratio ($\psi$) in the precursor. When $\psi$ is higher than 0.2 the decomposition of the Li–La–Ti–peroxocitrate salt is incomplete because the evolved heat in the exothermic effect at around 260 °C is not enough to provoke the complete transformation of the precursor in the $Li_{0.5}La_{0.5}TiO_3$ phase as it is shown in the XRD studies.

Fig. 4 shows the XRD patterns of the PCit-1 precursor ($\psi=\infty$) when heated from room temperature to 800 °C, accounting the changes during its transformation till the formation of the $Li_{0.5}La_{0.5}TiO_3$ phase. It is noticeable that the characteristic peaks of the perovskite phase are only observed after heating at temperatures over 600 °C. A different behavior is observed in the thermal transformation of citrate precursors prepared with the highest amount of $HNO_3$ (PCit-4 and PCit-5) as it is shown in Fig. 5. In both cases, the precursor is transformed into a single-crystalline $Li_{0.5}La_{0.5}TiO_3$ perovskite phase from 350 °C. In these last two cases the XRD diagrams show the presence of the expected fundamental peaks and with their relative intensities in well concordance with those reported in PDF 89-4928 for the cubic ($Pm\bar{3}m$) $Li_{0.5}La_{0.5}TiO_3$ composition. In these systems it can be also observed the presence of additional XRD peaks when the material is heated at temperatures above 600 °C, indicating the formation of secondary phases above such temperature. These observations support the idea that 350 °C seems to be the optimal temperature for the $Li_{0.5}La_{0.5}TiO_3$ composition phase formation when -citrate/nitrate combustion takes place affording in the process the necessary energy to induce the precursor transformation.

In the case of the PCit-2 and PCit-3 precursors, in which the $\psi$ parameter present values higher than those for PCit-4 and PCit-5 precursors, the XRD patterns (Fig. 6A and B, respectively) show the presence of the $Li_{0.5}La_{0.5}TiO_3$ phase but only after heating at 600 °C. These results point out to the role of the amount of $NH_4NO_3$ in the precursor because although this salt is also present in these precursors its concentration is not enough to produce as much energy in its decomposition at

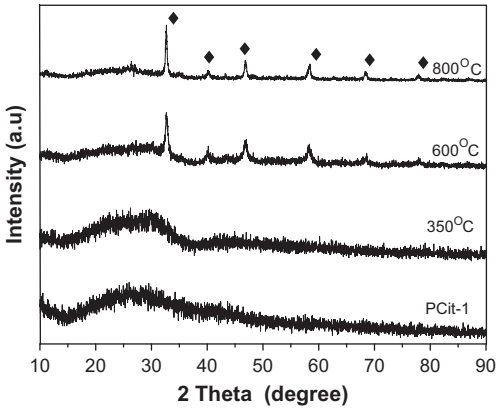


Fig. 4. XRD patterns of the PCit-1 precursor when heated from room temperature to 800 °C (♦) peaks ascribed to the $Li_{0.5}La_{0.5}TiO_3$ perovskite phase).

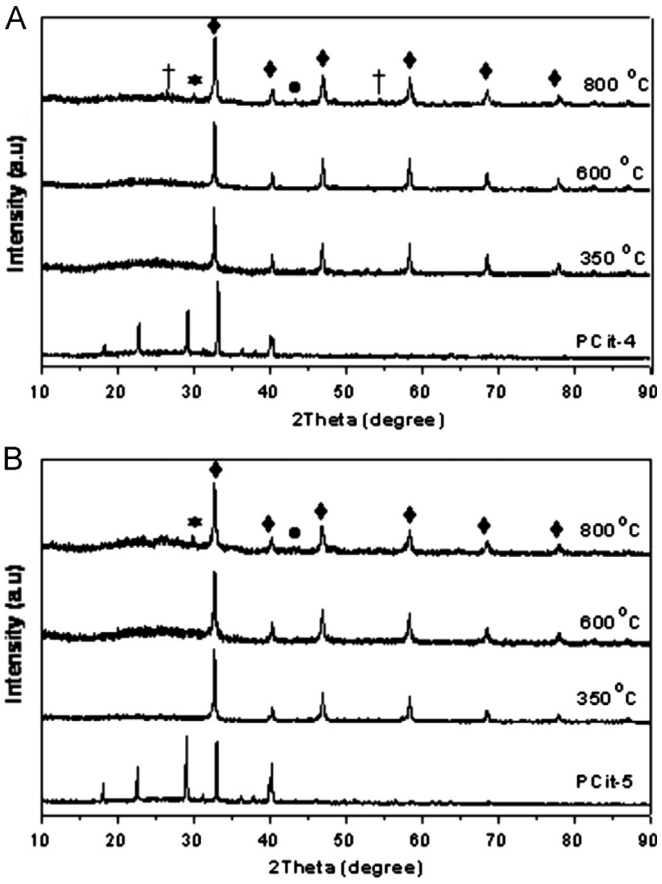


Fig. 5. XRD patterns of the PCit-4 (A) and PCit-5 (B) precursors when heated from room temperature to 800 °C. (♦) peaks ascribed to the $Li_{0.5}La_{0.5}TiO_3$ perovskite phase, $Li_2Ti_2O_5$ (●) [10], $TiO_2$ (†) and $La_2Ti_2O_7$ (*) impurities.

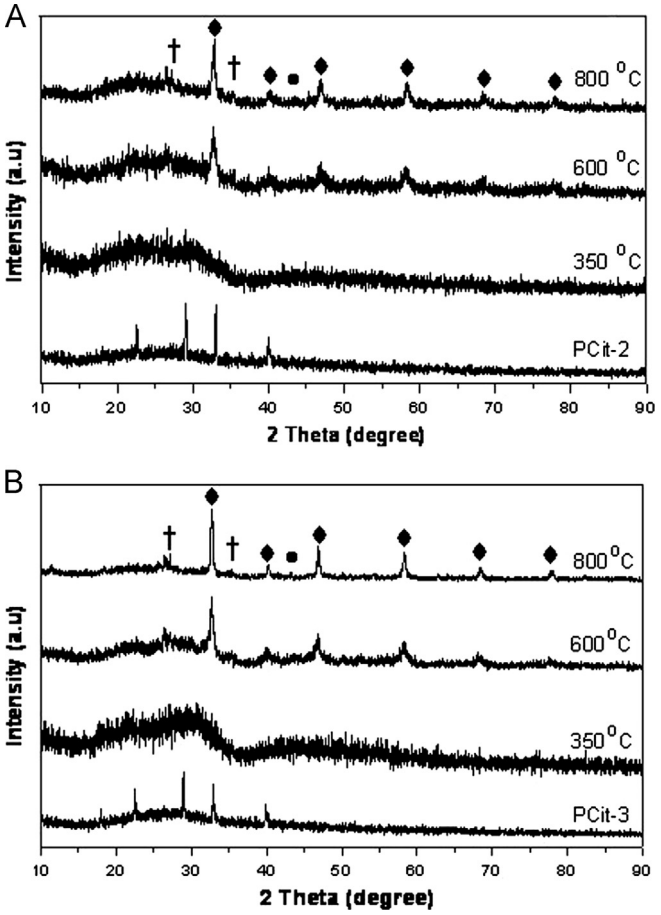


Fig. 6. XRD patterns of the PCit.2 (A) and PCit-3 (B) precursors when heated from room temperature to 800 °C. (♦) peaks ascribed to the $Li_{0.5}La_{0.5}TiO_3$ perovskite phase, $Li_2Ti_2O_5$ (●) and $TiO_2$ (†).

260 °C to provoke the transformation of the citrate precursor in to the desired LLTO phase.

From the propellants chemistry it is known that in a combustion reaction the most stable final products are metal oxides accompanied by evolved $CO_2$, $H_2O$ and $N_2$ molecules [17,36,37]. Bearing in mind this fact and considering the experimental results above discussed, it can be proposed the following redox citrate–nitrate reaction for the combustion system here reported:

$$Li_{0.5}La_{0.5}[Ti(\ O_2)(C_6H_4O_7)](s) + 8NH\ _4NO_3(s) \rightarrow$$

$$Li_{0.5}La_{0.5}TiO_3(s) + 18H\ _2O(g) + 6CO\ _2(g) + 8N\ _2(g)$$

From the redox equation it can be determined that the theoretical citrate/nitrate molar ratio is 1/8, i.e. 0.125, which is close to the calculated citrate/nitrate relation found in PCit-4 ($\Psi$=0.17) and PCit-5 ($\Psi$=0.13). Actually, these two citrate precursors are the two ones able to warrant the synthesis of the LLTO phase by the combustion reaction procuring the required Li(I), La(III) and Ti(IV) metal ions and with the $NH_4NO_3$ salt acting as the energy source and oxidant that provokes the combustion of the peroxocitrate salt (fuel). Moreover, the fact that the metal ions are present in the same molecule within atomic distances facilitates the kinetic of the solid state reaction for the LLTO phase formation without practically impurities at very low temperatures (350 °C).

A deeper analysis by HRTEM (Fig. 7) of the $Li_{0.5}La_{0.5}TiO_3$ material obtained from the PCit-5 precursor heated at 350 °C confirms the formation of this phase as nanoparticles with particle size ranging from 15 to 20 nm. This small particle size is due to the fact that during the reaction (see above equation) a huge quantity of gases is evolved (32 mol per each mole of oxide formed). It could be easily assumed that this mass of gases act as an impediment for the growing and aggregation of the resulting oxide particles. A zoom of the TEM image (inset in Fig. 7) allows the observation of the atomic planes in the crystal. Distances between these planes were calculated using the Gwyddion 2.23 program showing a value of 2.73 Å which is similar to the interplanar distance calculated from the most intense XRD peak of the $Li_{0.5}La_{0.5}TiO_3$ phase (Fig. 5B).

Due to the potential interest of this $Li_{0.5}La_{0.5}TiO_3$ phase obtained from PCit-5 precursor heated at 350 °C with the formation of the oxide as nanoparticles, the *ac* electric behavior of the material with temperature (100–300 °C) has been analyzed by EIS (Fig. 8). The typical response of this type of materials in ESI consists of two semicircles and a spike in the low frequency region. However, as it can be seen in Fig. 8 the impedance plot shows only one arc. This effect may be ascribed to the presence of particles of nanometer size [7,38,39] in which the surface processes predominate over the grain ones. The intercept of the semicircle with the abscises axis at high frequencies can be assumed as the grain resistance of the material. It can be also seen in Fig. 8 the associated equivalent circuit with a number of elements connecting in series and/or in parallel, where the resistance element ($R_g$) justifies the fact that the arcs do not begin at the origin of the graph and simulates the grain conduction of the LLTO oxide. The second block contains the information referred to the unique observed semicircle. The calculated grain boundary capacity ($C_{gb}$), was in all the cases of around 10 nF, which agrees well with the value reported for the assignation of grain boundaries processes. In parallel a grain

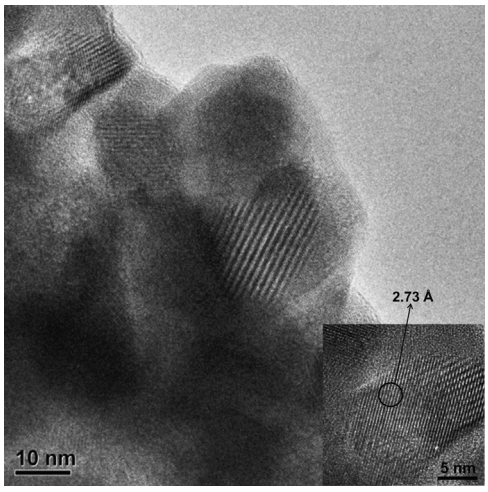


Fig. 7. HRTEM image of the $Li_{0.5}La_{0.5}TiO_3$ phase obtained from PCit-5 heated at 350 °C. The inset shows a magnification in which is possible to evaluate the interplanar atomic distance.

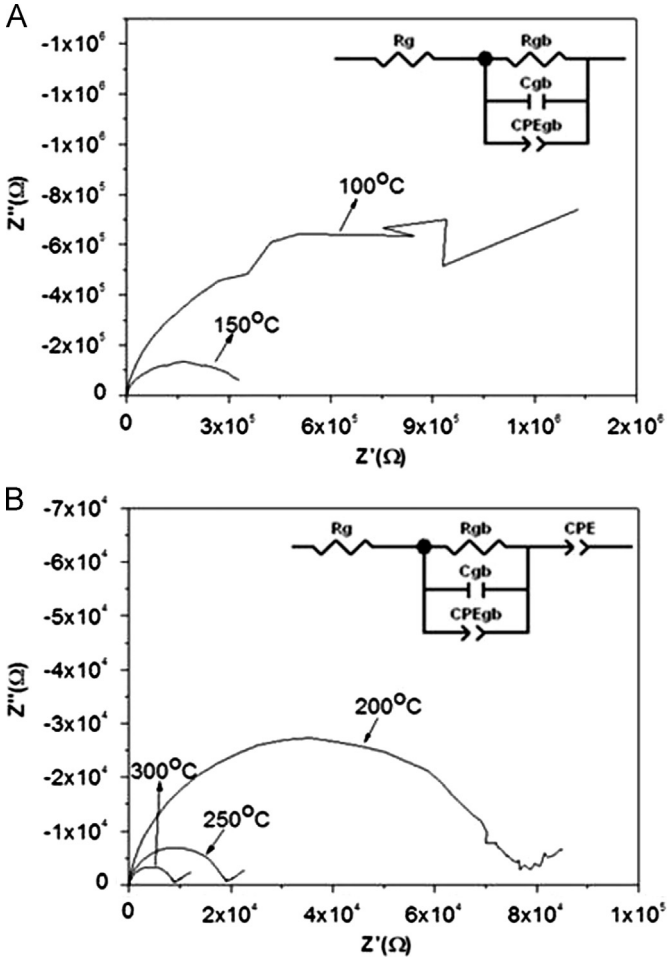


Fig. 8. Impedance plots and equivalent circuits in the 100–300 °C temperature range of the LLTO material obtained from PCit-5 heated at 350 °C.

boundary resistance element ($R_{gb}$) was added in these blocks which reproduces the conduction in the grain interface [40]. A grain boundary constant phase element ($CPE_{gb}$) in parallel was added because all the arcs are deformed and their centers are displaced above the real impedance axis, showing a non-Debye response. In the case of spectra registered above 200 °C the equivalent circuits contain a third block with a constant phase element (CPE). This CPE element reproduces the appearance of an inclined spike in the low frequency region due to the blocking effect of the electrodes.

Fig. 9 shows the Arrhenius plots for both the intra-grain and grain boundaries conductivities, $\sigma_g$ and $\sigma_{gb}$, respectively, deduced from the ESI curves in the 100–300 °C temperature range. By interpolation in those plots it can be estimated values of $\sigma_g$ equal to $1.33 \cdot 10^{-4}$ S cm$^{-1}$ and $\sigma_{gb}$ equal to$7.28 \cdot 10^{-10}$ S cm$^{-1}$ at room temperature. This $\sigma_g$ value agrees well with the one already reported for this composition [5]. However $\sigma_{gb}$ is significant below to the expected value at room temperature [5] as it grows markedly from $10^{-10}$ to $10^{-6}$ S/cm from room temperature to 300 °C. This divergence can be related to the fact that here the particles have been agglomerated by cold press, which may be not adequate for so small particles (10–20 nm) as the ones obtained by the method here reported. Further studies will be dedicated to the search of a more effective method to

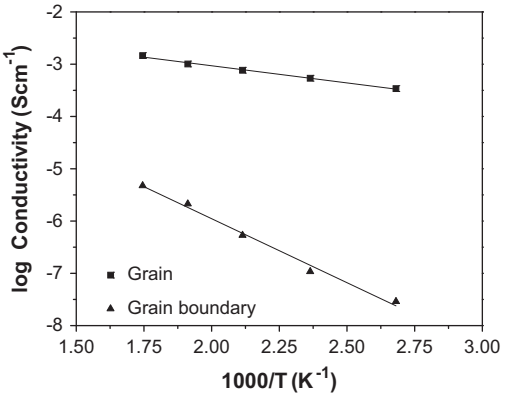


Fig. 9. Arrhenius plots for the LLTO material obtained from PCit-5 heated at 350 °C. Activation energies corresponding to grain (■) and grain boundary (▲) conductivities obtained from $\sigma_g$ and $\sigma_{gb}$, respectively, in the 100–300 °C temperature range.

reach the agglomeration of the particles in order to make use of the high conductivity detected in the bulk of this material.

## 4. Conclusions

A systematic investigation about the synthesis of nanocrystalline $Li_{0.5}La_{0.5}TiO_3$ phase powders by a nitrate–citrate redox reaction that implies combustion of the reagents has been carried out varying the nitrate content (oxidant) in the starting citrate precursor. In this way, the fuel composition contains $Li_{0.5}La_{0.5}Ti(O_2)(C_6H_4O_7)$ as precursor of the LLTO phase and variable amounts of ammonium nitrate. The nitrate–citrate molar ratio has a decisive influence on the formation of the LLTO phase. Two undesired effects, particle agglomeration and presence of inorganic impurities, are observed to become quite significant as the calcination temperature is increased from 350 °C to 800 °C. The theoretical optimum nitrate/citrate molar ratio for the synthesis of $Li_{0.5}La_{0.5}TiO_3$ phase crystals as nanoparticles without inorganic impurity was 0.125, which appear to be very close to the value of the molar ratio in the prepared PCit-5 precursor. The LLTO phase (cubic-$Li_{0.5}La_{0.5}TiO_3$) resulting from this precursor after heating at 350 °C are composed of nanoparticles of 15–20 nm and shows an impedance electric response typical of ionic nanostructured conducting material with conductivity values at room temperature of around $10^{-4}$ S cm$^{-1}$ inside the grain.

## Acknowledgments

This work has been partially supported by the CONACYT (Projects: # 129227, # 17424 and #148997) and SIP-IPN (Project: 20111101), CICYT (Spain project MAT2012- 31759) and CNPq-MES Project # 490522/2010-6.

## References

[1] M. Armand, J.M. Tarascon, Building better batteries, Nature 451 (2008).
[2] B. Scrosati, J. Garche, Lithium batteries: status, prospects and future, Journal of Power Sources 195 (2010) 2419–2430.

[3] P.G. Bruce, B. Scrosati, J.M. Tarascon, Nanomaterials for rechargeable lithium batteries, Angewandte Chemie International Edition 47 (2008) 2930–2946.
[4] N. Meethong, H.-Y.S. Huang, W.C. Carter, Y.-M. Chiang, Size-dependent lithium miscibility gap in nanoscale $Li_{1-x}FePO_4$, Electrochemical and Solid-State Letters 10 (2007) A134–A138.
[5] S. Stramare, V. Thangadurai, W. Weppner, Lithium lanthanum titanates: a review, Chemistry of Materials 15 (2003) 3974–3990.
[6] J.W. Fergus, Ceramic and polymeric solid electrolytes for lithium-ion batteries, Journal of Power Sources 195 (2010) 4554–4569.
[7] K. Kitaoka, H. Kozuka, T. Hashimoto, T. Yoko, Preparation of $La_{0.5}Li_{0.5}TiO_3$ perovskite thin films by the sol–gel method, Journal of Materials Science 32 (1997) 2063–2070.
[8] M. Vijayakumar, Q.N. Pham, C. Bohnke, Lithium lanthanum titanate ceramic as sensitive material for pH sensor: influence of synthesis methods and powder grains size, Journal of the European Ceramic Society 25 (2005) 2973–2976.
[9] M.P. Pechini, Method of Preparing Lead and Alkaline Titanates and Niobiates and Coating Method Using the Same to Form a Capacitor, USA, 1967, p. 697.
[10] M. Vijayakumar, Y. Inaguma, W. Mashiko, M.-P. Crosnier-López, C. Bhonke, Synthesis of fine powders of $Li_{3x}La_{2/3-x}TiO_3$ perovskite by a polymerizable precursor method, Chemistry of Materials 16 (2004) 2719–2724.
[11] Q.N. Pham, C. Bohnke, M.P.C. Lopez, O. Bohnke, Synthesis and characterization of nanostructured fast ionic conductor $Li_{0.30}La_{0.56}TiO_3$, Chemistry of Materials 18 (2006) 4385–4392.
[12] S.K. Behera, P. Barpanda, S.K. Pratihar, S. Bhattacharyya, Synthesis of magnesium–aluminium spinel from autoignition of citrate–nitrate gel, Materials Letters 58 (2004) 1451–1455.
[13] G.V.K.V. Werde, D. Mondelaers, H.D. Rul, M.K.V. Bael, J. Mullens, L. C.V. Poucke, The aqueous solution-gel synthesis of perovskite $Pb(Zr_{1-x}Ti_x)O_3$ (PZT), Journal of Materials Science 42 (2007) 624–632.
[14] R.D. Purohit, S. Saha, A.K. Tyagi, Nanocrystalline thoria powders via glycine–nitrate combustion, Journal of Nuclear Materials 288 (2001) 7–10.
[15] N. Chakrabarti, H.S. Maiti, Chemical synthesis of PZT powder by autocombustion of citrate–nitrate gel, Materials Letters 30 (1997) 169–173.
[16] M. Marinsek, K. Zupan, J. Maeek, Ni–YSZ cermet anodes prepared by citrate/nitrate combustion synthesis, Journal of Power Sources 106 (2002) 178–188.
[17] S.R. Jain, K.C. Adiga, V.R.P. Verneker, A new approach to thermochemical calculations of condensed fuel–oxidizer mixtures, Combustion and flame 40 (1981) 71–79.
[18] K. Zupan, D. Kolar, M. Marinsek, Influence of citrate–nitrate reaction mixture packing on ceramic powder properties, Journal of Power Sources 86 (2000) 417–422.
[19] P. Folly, P. Mädera, Propellant chemistry, CHIMIA International Journal for Chemistry 58 (2004) 374–382.
[20] K.A. Singh, L.C. Pathak, S.K. Roy, Effect of citric acid on the synthesis of nano-crystalline yttria stabilized zirconia powders by nitrate–citrate process, Ceramics International 33 (2007) 1463–1468.
[21] T. Otero, Y. Mosqueda, C.R. Miilian, E Perez-Cappe, $Li_{3x}La_{2/3-x}TiO_3$ nanoparticles obtained from a low temperature synthesis route, Journal of Nano Research 14 (2011) 107–113.
[22] A. Théoret, C. Sandorfy, Infrared spectra and crystalline phase transitions of ammonium nitrate, Canadian Journal of Chemistry 42 (1964) 57–62.
[23] R.S.E. Zhecheva, M. Gorova, R. Alcántara, J. Morales, J.L. Tirado, Lithium–cobalt citrate precursors in the preparation of intercalation electrode materials, Chemistry of Materials 8 (1996) 1429–1440.
[24] D.S. Todorovsky, M.M. Getsova, I. Wawer, P. Stefanov, V. Enchev, On the chemical nature of lanthanum–titanium citric complexes, precursors of $La_2Ti_2O_7$, Materials Letters 58 (2004) 3559–3563.
[25] M. Dakanali, E.T. Kefalas, C.P. Raptopoulou, A. Terzis, G. Voyiatzis, I. Kyrikou, T. Mavromoustakos, A. Salifoglou, A new dinuclear Ti(IV)–peroxo–citrate complex from aqueous solutions. synthetic, structural, and spectroscopic studies in relevance to aqueous titanium(IV)–peroxo–citrate speciation, Inorganic Chemistry 42 (2003) 4632–4639.
[26] J. Muhlebach, K. Muller, G. Schawarzenbach, The peroxo complexes of titanium, Inorganic Chemistry 9 (1970) 2381–2390.
[27] A. Hardy, J. D'Haen, M.K.V. Bael, J. Mullens, An aqueous solution gel citratoperoxo Ti(IV) precursor: synthesis, gelation, thermo oxidative decomposition and oxide crystallization, Journal of Sol–Gel Science and Technology 44 (2007) 65–74.
[28] M. Kakihana, M. Kobayashi, K. Tomita, V. Petrykin, Application of water soluble titanium complexes as precursors for synthesis of titanium containing oxides via aqueous solution processes, Bulletin of the Chemical Society of Japan 83 (2010) 1285–1308.
[29] Y. Mosqueda, E.P. Cappe, P. Aranda, E. Ruiz-Hitzky, Preparation of an $Li_{0.7}Ni_{0.8}Co_{0.2}O_2$ electrode material from a new Li–Co–Ni mixed-citrate precursor, European Journal of Inorganic Chemistry (2005) 2698–2705.
[30] I. Bretos, R. Jiménez, M.L. Calzada, M.K.V. Bael, A. Hardy, D. V. Genechten, J. Mullens, Entirely aqueous solution−gel route for the preparation of $(Pb_{1-x}Ca_x)TiO_3$ thin films, Chemistry of Materials 18 (2006) 6448–6456.
[31] D.S. Todorovsky, M.M. Getsova, M.A. Vasileva, Thermal decomposition of lanthanum–titanium citric complexes prepared from ethylene glycol medium, Journal of Materials Science 37 (2002) 4029–4039.
[32] J.C. Oxley, J.L. Smith, E. Rogers, M. Yu, Ammonium nitrate: thermal stability and explosivity modifier, Thermochimica Acta 384 (2002) 23–45.
[33] C. Oommen, S.R. Jain, Ammonium nitrate: a promising rocket propellant oxidizer, Journal of Hazardous Materials 67 (1999) 253–281.
[34] R.C. Korošec, P. Kajič, P. Bukovec, Determination of water, ammonium nitrate and sodium nitrate content in 'water-in-oil' emulsions using TG and DSC, Journal of Thermal Analysis and Calorimetry 89 (2007) 619–624.
[35] S. Banerjee, A. Kumar, P.S. Devi, Preparation of nanoparticles of oxides by the citrate–nitrate process. Effect of metal ions on the thermal decomposition characteristics, Journal of Thermal Analysis and Calorimetry (2011).
[36] K.C. Patil, M.S. Hegde, Tanu Rattan, S.T. Aruna, Chemistry of Nanocrystalline Oxide Materials: Combustion Synthesis, Properties and ApplicationsWorld Scientific Publishing Co. Pvt. Ltd., Singapore, 2008.
[37] J. Akhavan, The Chemistry of Explosives, in: R.S.o. Chemistry (Ed.), 2004.
[38] C.H. Chen, K. Amine, Ionic conductivity, lithium insertion and extraction of lanthanum lithium titanate, Solid State Ionics 144 (2001) 51–57.
[39] Evegenij Barsoukov, in: Evegenij Barsoukov, J. Ross Macdonald (Eds.), Impedance Spectroscopy: Theory, Experiment and Applications, second edition, John Wiley & Sons, Inc., New Jersey, 2005.
[40] H.-T. Chung, J.-G. Kim, H.-G. Kim, Dependence of the lithium ionic conductivity on the B-site ion substitution in $(Li_{0.5}\ La_{0.5})Ti_{1-x}M_xO_3$ (M = Sn, Zr, Mn, Ge), Solid State Ionics 107 (1998) 153–160.